Immobilizing Highly Catalytically Active Pt Nanoparticles inside the Pores of Metal−Organic Framework: A Double Solvents Approach

Arshad Aijaz,[†] Abhi Karkamkar,[‡] Young Joon Choi,[‡] Nobuko Tsumori,[§] Ewa Rönnebro,[‡] Tom Autrey,[‡] Hiroshi Shioyama,[†] and Qiang Xu*,[†]

[†]National Institute of Advanced Industrial Science and Technology (AIST), Ikeda, Osaka 563-8577, Japan
[‡]Pacific Northwest National Laboratory (PNNL), Richland, Washington 99352, United States
[§]Toyama National College of Technology, 13, Hongo-machi, Toyama, 939-8630, Japan

Ⓢ Supporting Information

ABSTRACT: Ultrafine Pt nanoparticles were successfully immobilized inside the pores of a metal−organic framework, MIL-101, without aggregation of Pt nanoparticles on the external surfaces of framework by using a "double solvents" method. TEM and electron tomographic measurements clearly demonstrated the uniform three-dimensional distribution of the ultrafine Pt NPs throughout the interior cavities of MIL-101. The resulting Pt@MIL-101 composites represent the first highly active MOF-immobilized metal nanocatalysts for catalytic reactions in all three phases: liquid-phase ammonia borane hydrolysis, solid-phase ammonia borane thermal dehydrogenation, and gas-phase CO oxidation.

Catalysis using metal nanoparticles (MNPs) has attracted great interest in recent years.[1] Considering the current impetus of nanoscience, it is understandable that all the aspects related to the preparation of small nanoparticles (NPs) with narrow size distribution, their stabilization and their unique properties compared to larger particles are appealing to a large community of researchers from materials science, computational chemistry, catalysis and so on.[2] Nanostructured and nanoscale materials strongly offer the possibility of controlling material tailoring parameters independently of their bulk counterparts.[3]

Porous metal−organic frameworks (MOFs) have emerged as a class of very promising hybrid functional materials.[4] Over the past decades, research efforts have been mostly aimed in preparing new MOF structures and studying their applications in molecule storage and separation.[5] Loading of MNPs inside the porous matrices of MOFs is of current interest.[6−11] There have been two approaches for the synthesis of MNPs inside MOFs. The first and most widely used approach is to use MOFs as stabilizing host material providing a confined space for nucleation, which includes techniques such as chemical vapor deposition,[7] solution infiltration,[8] and solid grinding[9] for introducing the metal precursor. A recent report has demonstrated the use of a photoactive MOF as matrix to generate metal microstructures within the framework by photoreduction of the metal precursors introduced by solution infiltration.[10a] The second approach, reported very recently,[11] involves synthesis of MNPs individually first and subsequent

addition of suitable chemicals to construct the MOF around the MNPs. Although great efforts have been made in this field, a general and facile method is still needed that can easily introduce all the metal precursor inside the cavities of MOF and control the formation of ultrafine MNPs with a small particle size, which is beneficial in cases such as catalysis, inside the cavities without aggregation on the external surfaces of MOF. Herein, we report the use of "double solvents" method for the first time to introduce ultrafine Pt NPs into MOF nanopores without Pt NPs aggregation on the external surface of framework, which exhibit excellent catalytic performances for liquid-phase (ammonia borane hydrolysis), solid-phase (ammonia borane thermal dehydrogenation) and gas-phase (CO oxidation) reactions.

MIL-101,[12] a chromium-based MOF with molecular formula $Cr_3F(H_2O)_2O[(O_2C)C_6H_4(CO_2)]_3 \cdot nH_2O$ (where n is ~25), was chosen for this strategy because of its high stability in water, large surface area, and two hydrophilic zeotypic cavities with free diameters of ca. 2.9 and 3.4 nm accessible through two pore windows of ca. 1.2 and 1.6 nm in diameter. These pore windows are big enough for the metal precursor H_2PtCl_6 to diffuse into the cavities, within which nucleation can take place to form Pt NPs (Figure 1). The "double solvents" method[13]
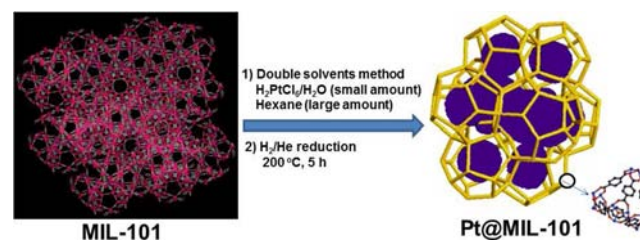

Figure 1. Schematic representation of synthesis of Pt nanoparticles inside the MIL-101 matrix using double solvents method.

used in this work for avoiding MNPs aggregation on external surfaces of MIL-101 framework is based on a hydrophilic solvent (water) and a hydrophobic solvent (hexane), the former containing the metal precursor with a volume set equal to or less than the pore volume of the adsorbent (MIL-101), which can be absorbed within the hydrophilic adsorbent pores,

and the latter, in a large amount, playing an important role to suspend the adsorbent and facilitate the impregnation process. Since the inner surface area of MIL-101 is much larger than the outer surface area, the small amount of aqueous H_2PtCl_6 (equal or less than pore volume) could go inside the hydrophilic pores by capillary force, which greatly minimizes the deposition of H_2PtCl_6 on the outer surface. In contract, in the conventional single-solvent impregnation process, a large amount of solvent containing the metal precursor is used, some of which will be deposited on the outer surfaces of MOF after drying, generating aggregated MNPs on the outer surfaces.

MIL-101 was obtained following the synthesis procedure described in the literature.[12,14] For loading Pt inside the cavities of MIL-101, 100 mg of green MIL-101 powder activated by heating at 150 °C for 12 h under dynamic vacuum, which has a pore volume of 2.01 cm^3 g^{-1} as determined by N_2 sorption isotherm, was suspended in dry n-hexane (20 mL), to which an aqueous H_2PtCl_6 solution (0.20 mL) with different concentrations was added dropwise under continuous vigorous stirring. After careful filtration, the green powder was dried in air at room temperature. These synthesized samples were further dried at 150 °C for 12 h, followed by treating in a stream of H_2/He (50 mL min^{-1}/50 mL min^{-1}) at 200 °C for 5 h to yield Pt@MIL-101. During the reduction, there was no color change in the samples, suggesting that the formed Pt NPs are highly dispersed within the MIL-101 cavities. There was no loss of crystallinity in the powder X-ray diffraction (PXRD) patterns after H_2 reduction for Pt@MIL-101 with Pt loadings up to 5 wt %, suggesting that the integrity of the MIL-101 framework is maintained (Figure S1). The PXRD pattern of Pt@MIL-101 did not exhibit the characteristic peaks for Pt, indicating the formation of very small NPs. The large decrease in the amount of N_2 adsorption and the pore volume of Pt@MIL-101 indicates that the cavities of the MIL frameworks are occupied by the highly dispersed Pt NPs (Figure S2). The X-ray photoelectron spectroscopic (XPS) investigation of Pt@MIL-101 at the Pt 4f levels exhibited metallic Pt(0) peaks (Figure S3).

The high-angle annular dark-field scanning TEM (HAADF-STEM), bright field-STEM (BF-STEM), TEM images (Figures 2, S4 and S5), energy-dispersive X-ray spectroscopy (EDX) analyses (Figure S6) and electron tomographic reconstruction
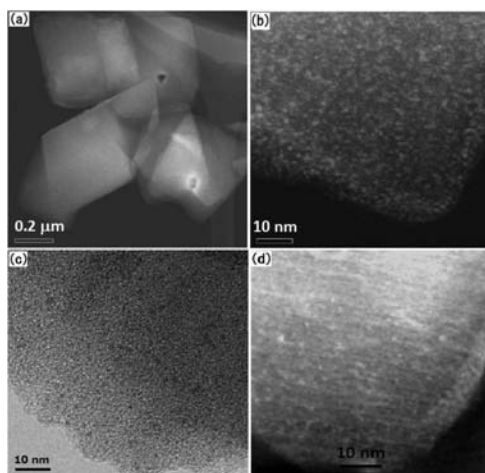
(Figure 2d and a movie provided as Supporting Information)[14] of 2 wt % Pt@MIL-101 exhibited the uniformity of the Pt NPs in the MIL-101 framework. The TEM images showed that the sizes of the Pt NPs were in the range of 1.2–3.0 nm with average size of 1.8 ± 0.2 nm (Figure S7), which are small enough to be accommodated in the two mesoporous cavities of MIL-101. Differently from the previous reports,[6−10] these TEM images showed no big particle aggregation. HRTEM analysis and diffraction patterns showed that the Pt NPs are crystalline with a spacing of 2.4 Å corresponding to Pt(1 1 1) (Figure S8). Electron tomographic reconstruction clearly demonstrated the uniform three-dimensional distribution of ultrafine Pt NPs throughout the interior cavities of MIL-101 crystals.[14]

It is well-known that the catalytic activity generally increases with the decrease of MNP size, as smaller MNPs have higher surface areas available for reactants. Therefore, these completely confined ultrafine MNPs into MIL-101 could be as model catalyst for different catalytic reactions. Interestingly, the highly dispersed Pt NPs inside MIL-101 exhibited excellent catalytic activities for reactions in all three phases, that is, liquid-phase ammonia borane hydrolysis, solid-phase ammonia borane thermal dehydrogenation, and gas-phase CO oxidation reactions. One more benefit of using MIL-101 as host for MNPs, which has cavities (2.9 and 3.4 nm) larger than the open windows (1.2 and 1.6 nm), is the size limitation effect of the windows, which prevent the NPs (mean size, 1.8 ± 0.2 nm) from crossing the framework. Therefore, reactants can access the reactive MNPs but MNPs cannot diffuse outside from the cavities, which consequently minimizes the possibility of agglomeration of MNPs even in liquid-phase catalysis.

It is well-known that ammonia borane (NH_3BH_3, AB) is a promising material for chemical hydrogen storage, from which H_2 can be released through either hydrolysis or pyrolysis.[15,16] First, the obtained Pt@MIL-101 was tested for the catalytic hydrolysis of ammonia borane. The reaction was initiated by introducing aqueous AB solution into the reaction flask containing the as-synthesized Pt@MIL-101 catalyst with vigorous shaking at room temperature.[14] Figures 3 and S9

Figure 2. (a, b) HAADF-STEM, (c) TEM images and (d) reconstructed slice by tomography of 2 wt % Pt@MIL-101.
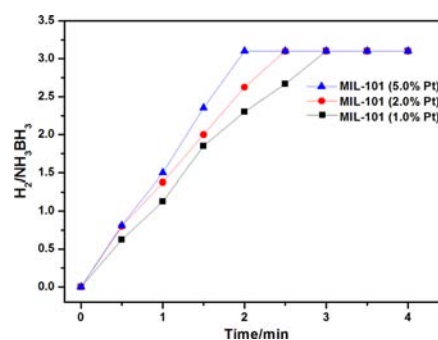

Figure 3. Hydrogen generation from aqueous NH_3BH_3 in the presence of Pt@MIL-101 catalysts at room temperature. Pt/AB (molar ratio) = 0.0014, 0.0029, and 0.0071 at Pt loadings of 1.0, 2.0 and 5.0%, respectively.

show the H_2 generation from aqueous AB at room temperature in the presence of Pt@MIL-101 with different Pt loadings. It is revealed that all the Pt@MIL-101 catalysts are highly active for the hydrolysis of AB, exhibiting hydrogen release of H_2/AB = 3. With 2 wt % Pt@MIL-101 (Pt/AB = 0.0029 in molar ratio), the hydrolysis of AB is completed within 2.5 min, corresponding to $\sim 1.0 \times 10^4$ L_{H2} mol_{Pt}^{-1} min^{-1}, 2 times higher than that of 2 wt

% Pt/γ-Al$_2$O$_3$, the most active Pt catalyst for this reaction reported so far.[15j] Reasonably, the small sizes of Pt NPs within MIL-101 account for the observed high catalytic activity. It is found that the productivity of H$_2$ over the Pt@MIL-101 catalysts remains unchanged after five runs, indicating the high durability in AB hydrolysis (Figure S10). PXRD (Figure S11) and TEM (Figure S12) measurements of Pt@MIL-101 after AB hydrolysis showed no significant changes in the morphologies of Pt NPs with retention of the MIL-101 framework.[14] Since the biproduct (BO$_2^-$) formed in AB hydrolysis is soluble in water, we can remove the spent fuels by water washing and reuse the catalyst.

Pyrolysis is another route to H$_2$ release from AB. It has been reported that confinement of AB in nanoscaffolds can improve the kinetics of the dehydrogenation of AB and suppress the emission of undesired volatile byproducts.[16] In addition to the nanoconfinement, MNP catalysts within the nanospace can hopefully superpose effects for improving H$_2$ release from AB. In this regard, we tested the dehydrogenation performance of AB in the pores of Pt@MIL-101. Liquid NH$_3$ was used as solvent to load AB into MIL-101 and 1% Pt@MIL-101 with 1:1 wt/wt to form the AB@MIL-101 and AB/Pt@MIL-101 composites. Temperature-programmed desorption mass spectrometry (TPS/MS) was used to compare the temperature profiles of volatile products (H$_2$, NH$_3$ and B$_3$N$_3$H$_6$) released from pristine AB and the AB@MIL-101 and AB/Pt@MIL-101 composites (Figure 4). The pristine AB released the first
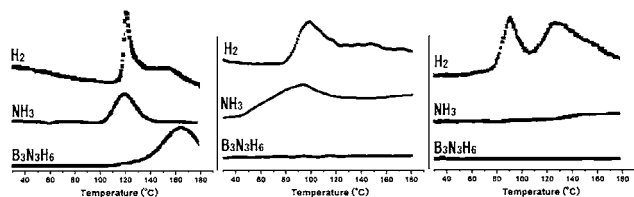

Figure 4. TPD-MS spectra of pristine AB (left), AB@MIL-101 (AB/MIL-101 = 1:1 wt/wt) (middle), and AB/Pt@MIL-101 (AB/1% Pt@MIL-101 = 1:1 wt/wt) (right).

equivalent of H$_2$ around 120 °C and the second equivalent of H$_2$ at 160 °C accompanied by a large evolution of borazine at around 140–200 °C, which is consistent with the reported results.[16] Compared to pristine AB, AB@MIL-101 started to evolve H$_2$ at 70 °C with a broad peak centered at 95 °C. The evolution of ammonia was not completely suppressed, while no borazine was detected. Interestingly, in the case of AB/Pt@MIL-101, the dehydrogenation temperature shifted to lower temperature. The AB/Pt@MIL-101 sample showed the first and second H$_2$ evolution peaks at about 88 and 130 °C, respectively, which are ~30 °C lower than those for the pristine AB. No noticeable peaks corresponding to NH$_3$ and borazine were detected. The thermogravimetric analysis (TG) results showed that the weight losses of the AB@MIL-101 and AB/Pt@MIL-101 decreased compared to that of the pristine AB (Figure S13). For AB/Pt@MIL-101, the total weight loss by 180 °C is 6.5 wt %, corresponding to the theoretical value of 2 equivs H$_2$ release (6.53 wt %), suggesting a significant suppression of the volatile byproducts. Notably, for both AB@MIL-101 and AB/Pt@MIL-101, no material foaming and expansion were observed during the AB decomposition.[16f] After pyrolysis, the crystallinity of the Pt@MIL-101 host matrix as well as Pt particle size remains unchanged as confirmed by the TEM images (Figure S14) and PXRD patterns (Figure S15).[14]

The lowering of AB dehydrogenation temperature and the effective depression of volatile byproducts and material foaming observed for AB/Pt@MIL-101 clearly demonstrate the synergetic effect of the Pt NPs catalysis and nanoconfinement of MIL-101 framework.

To assess the catalytic functionality of the ultrafine Pt NPs immobilized within MIL-101 for gas-phase reactions, we carried out the CO oxidation reaction[17] from room to elevated temperatures. The reaction was performed using a fixed bed flow reactor. Figure 5 shows the CO conversion as a function of
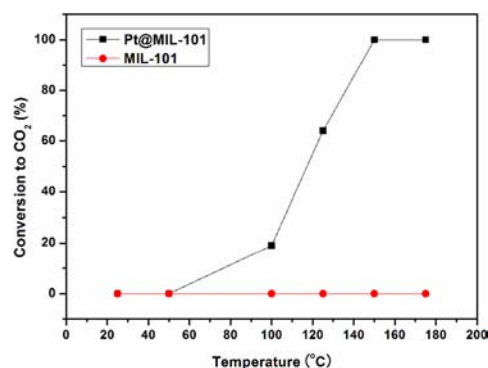

Figure 5. Conversion of CO over MIL-101 and 5% Pt@MIL-101 catalysts as a function of temperature (CO/O$_2$/He = 1:20:79, 20 000 mL h^{-1} g$_{cat.}^{-1}$).

temperature. MIL-101 exhibited no catalytic activity for CO oxidation reaction in the whole temperature range. The 5% Pt@MIL-101 started to show the activity at 50 °C, while CO to CO$_2$ conversion increased suddenly at 100 °C with complete conversion at 150 °C. Arrhenius plots show that the activation energy is 40.7 kJ mol^{-1} (Figure S17), which is comparable to the reported values of the mesoporous silica supported Pt catalyst.[18] The catalyst showed stable activity, keeping 100% CO conversion for 150 min at 175 °C (Figure S18). After catalytic reaction, the crystallinity of the Pt@MIL-101 host matrix remains unchanged with no large Pt particle aggregation as confirmed by the TEM measurements (Figure S19) and PXRD patterns (Figure S20).[14] The small sizes of the MNPs stably incorporated within MIL-101 pores largely contribute to the high activity, as observed previously for M@MIL-101 (M = Pd, Cu) catalysts.[10c]

In conclusion, we have developed a facile, general and effective "double solvents" approach for the incorporation of MNPs within pores of metal−organic frameworks without deposition of the MNPs on the external surface of host framework. We have used this efficient method for the first time to generate ultrafine Pt NPs inside the mesoporous MOF, MIL-101, which exhibit excellent catalytic performances for reactions in all phases of liquid, solid and gas. Uniform distribution of Pt NPs without aggregation after catalysis confirms the advantage of MNPs within the MIL-101 matrix. The present results bring light to new opportunities in the development of high-performance heterogeneous catalysts by using functionalized cavities of MOFs as hosts for ultrafine MNPs.

■ ASSOCIATED CONTENT

⑤ Supporting Information
Experimental procedures; PXRD, HAADF-STEM, TEM, XPS, and EDX for Pt@MIL-101; results of catalytic AB hydrolysis; TG results for AB, AB@MIL-101 and AB/Pt@MIL101;

Arrhenius plot for CO oxidation. This material is available free of charge via the Internet at http://pubs.acs.org.

■ AUTHOR INFORMATION

Corresponding Author
q.xu@aist.go.jp
Notes
The authors declare no competing financial interest.

■ ACKNOWLEDGMENTS

■ REFERENCES

(1) (a) Zhang, H.; Watanabe, T.; Okumura, M.; Haruta, M.; Toshima, N. *Nat. Mater.* **2012**, *11*, 49. (b) White, R. J.; Luque, R.; Budarin, V. L.; Clark, J. H.; Macquarrie, D. J. *Chem. Soc. Rev.* **2009**, *38*, 481. (c) Turner, M.; Golovko, V. B.; Vaughan, O. P. H.; Abdulkin, P.; Berenguer-Murcia, A.; Tikhov, M. S.; Johnson, B. F. G.; Lambert, R. M. *Nature* **2008**, *454*, 981.

(2) (a) Chou, N. H.; Ke, X.; Schiffer, P.; Schaak, R. E. *J. Am. Chem. Soc.* **2008**, *130*, 8140. (b) Tao, A. R.; Habas, S.; Yang, P. *Small* **2008**, *4*, 310. (c) Schlögl, R.; Hamid, S. B. A. *Angew. Chem., Int. Ed.* **2004**, *43*, 1628.

(3) Den Breejen, J. P.; Radstake, P. B.; Bezemer, G. L.; Bitter, J. H.; Frøseth, V.; Holmen, A.; De Jong, K. P. *J. Am. Chem. Soc.* **2009**, *131*, 7197.

(4) (a) Cui, Y.; Yue, Y.; Qian, G.; Chen, B. *Chem. Rev.* **2012**, *112*, 1126. (b) Mulfort, K. L.; Hupp, J. T. *J. Am. Chem. Soc.* **2007**, *129*, 9604. (c) Huang, X. C.; Lin, Y. Y.; Zhang, J. P.; Chen, X. M. *Angew. Chem., Int. Ed.* **2006**, *45*, 1557. (d) Latroche, M.; Surblé, S.; Serre, C.; Mellot-Draznieks, C.; Llewellyn, P. L.; Lee, J.-H.; Chang, J.-S.; Jhung, S. H.; Férey, G. *Angew. Chem., Int. Ed.* **2006**, *45*, 8227. (e) Wu, C. D.; Hu, A.; Zhang, L.; Lin, W. *J. Am. Chem. Soc.* **2005**, *127*, 8940. (f) Kitagawa, S.; Kitaura, R.; Noro, S. *Angew. Chem., Int. Ed.* **2004**, *43*, 2334. (g) Seo, J. S.; Whang, D.; Lee, H.; Jun, S. I.; Oh, J.; Jeon, Y. J.; Kim, K. *Nature* **2000**, *404*, 982.

(5) (a) Zhang, H.-X.; Wang, F.; Yang, H.; Tan, Y.-X.; Zhang, J.; Bu, X. *J. Am. Chem. Soc.* **2011**, *133*, 11884. (b) Vermoortele, F.; Maes, M.; Moghadam, P. Z.; Lennox, M. J.; Ragon, F.; Boulhout, M.; Biswas, S.; Laurier, K. G. M.; Beurroies, I.; Denoyel, R.; Roeffaers, M.; Stock, N.; Düren, T.; Serre, C.; De Vos, D. E. *J. Am. Chem. Soc.* **2011**, *133*, 18526. (c) Furukawa, H.; Ko, N.; Go, Y. B.; Aratani, N.; Choi, S. B.; Choi, E.; Yazaydin, A. O.; Snurr, R. Q.; O'Keeffe, M.; Kim, J.; Yaghi, O. M. *Science* **2010**, *329*, 424. (d) Yang, S.; Lin, X.; Blake, A. J.; Walker, G. S.; Hubberstey, P.; Champness, N. R.; Schröder, M. *Nat. Chem.* **2009**, *1*, 487. (e) Cairns, A. J.; Perman, J. A.; Wojtas, L.; Kravtsov, V. C.; Alkordi, M. H.; Eddaoudi, M.; Zaworotko, M. J. *J. Am. Chem. Soc.* **2008**, *130*, 1560. (f) Dincă, M.; Long, J. R. *J. Am. Chem. Soc.* **2007**, *129*, 11172. (g) Wang, X. S.; Ma, S. Q.; Sun, D. F.; Parkin, S.; Zhou, H.-C. *J. Am. Chem. Soc.* **2006**, *128*, 16474.

(6) (a) Dhakshinamoorthy, A.; Garcia, H. *Chem. Soc. Rev.* **2012**, *41*, 5262. (b) Meilikhov, M.; Yusenko, K.; Esken, D.; Turner, S.; Tendeloo, G. V.; Fischer, R. A. *Eur. J. Inorg. Chem.* **2010**, *24*, 3701.

(7) (a) Park, Y. K.; Choi, S. B.; Nam, H. J.; Jung, D.-Y.; Ahn, H. C.; Choi, K.; Furukawa, H.; Kim, J. *Chem. Commun.* **2010**, *46*, 3086. (b) Esken, D.; Turner, S.; Lebedev, O. I.; Tendeloo, G. V.; Fischer, R. A. *Chem. Mater.* **2010**, *22*, 6393. (c) Schröder, F.; Esken, D.; Cokoja, M.; van den Berg, M. W. E.; Lebedev, O. I.; Tendeloo, G. V.; Walaszek, B.; Buntkowsky, G.; Limbach, H.-H.; Chaudret, B.; Fischer, R. A. *J. Am. Chem. Soc.* **2008**, *130*, 6119. (d) Proch, S.; Herrmannsdörfer, J.; Kempe, R.; Kern, C.; Jess, A.; Seyfarth, L.; Senker, L. *Chem.—Eur. J.* **2008**, *14*, 8204. (e) Hermes, S.; Schröter,

M.-K.; Schmid, R.; Khodeir, L.; Muhler, M.; Tissler, A.; Fischer, R. W.; Fischer, R. A. *Angew. Chem., Int. Ed.* **2005**, *44*, 6237.

(8) (a) Wang, C.; Dekrafft, K. E.; Lin, W. *J. Am. Chem. Soc.* **2012**, *134*, 7211. (b) Li, H.; Zhu, Z.; Zhang, F.; Xie, S.; Li, H.; Li, P.; Zhou, X. *ACS Catal.* **2011**, *1*, 1604. (c) Park, T.-H.; Hickman, A. J.; Koh, K.; Martin, S.; Wong-Foy, A. G.; Sanford, M. S.; Matzger, A. J. *J. Am. Chem. Soc.* **2011**, *133*, 20138. (d) Jiang, H. L.; Akita, T.; Ishida, T.; Haruta, M.; Xu, Q. *J. Am. Chem. Soc.* **2011**, *133*, 1304. (e) Zlotea, C.; Campesi, R.; Cuevas, F.; Leroy, E.; Dibandjo, P.; Volkringer, C.; Loiseau, T.; Férey, G.; Latroche, M. *J. Am. Chem. Soc.* **2010**, *132*, 2991. (f) Henschel, A.; Gedrich, K.; Kraehnert, R.; Kaskel, S. *Chem. Commun.* **2008**, 4192. (g) Hwang, Y. K.; Hong, D.-Y.; Chang, J.-S.; Jhung, S. H.; Seo, Y.-K.; Kim, J.; Vimont, A.; Daturi, M.; Serre, C.; Férey, G. *Angew. Chem., Int. Ed.* **2008**, *47*, 4144.

(9) (a) Jiang, H.-L.; Liu, B.; Akita, T.; Haruta, M.; Sakurai, H.; Xu, Q. *J. Am. Chem. Soc.* **2009**, *131*, 11302. (b) Ishida, T.; Nagaoka, M.; Akita, T.; Haruta, M. *Chem.—Eur. J.* **2008**, *14*, 8456.

(10) (a) Ameloot, R.; Roeffaers, M. B. J.; De Cremer, G.; Vermoortele, F.; Hofkens, J.; Sels, B. F.; De Vos, D. E. *Adv. Mater.* **2011**, *23*, 1788. (b) Cheon, Y. E.; Suh, M. P. *Angew. Chem., Int. Ed.* **2009**, *48*, 2899. (c) Samy El-Shall, M.; Abdelsayed, V.; Khder, A. S.; Hassan, H. M. A.; El-Kaderi, H. M.; Reich, T. E. *J. Mater. Chem.* **2009**, *19*, 7625.

(11) Lu, G.; Li, S. Z.; Guo, Z.; Farha, O. K.; Hauser, B. G.; Qi, X. Y.; Wang, Y.; Wang, X.; Han, S. Y.; Liu, X. G.; DuChene, J. S.; Zhang, H.; Zhang, Q. C.; Chen, X. D.; Ma, J.; Loo, S. C. J.; Wei, W. D.; Yang, Y. H.; Hupp, J. T.; Huo, F. W. *Nat. Chem.* **2012**, *4*, 310.

(12) Férey, G.; Mellot-Draznieks, C.; Serre, C.; Millange, F.; Dutour, J.; Surblé, S.; Margiolaki, I. *Science* **2005**, *309*, 2040.

(13) Imperor-Clerc, M.; Bazin, D.; Appay, M.-D.; Beaunier, P.; Davidson, A. *Chem. Mater.* **2004**, *16*, 1813.

(14) See the Supporting Information.

(15) (a) Sanyal, U.; Demirci, U. B.; Jagirdar, B. R.; Miele, P. *ChemSusChem* **2011**, *4*, 1731. (b) Thomas, H.; Monika, H.; Dieter, L. *Chem.—Eur. J.* **2011**, *17*, 10184. (c) Jiang, H.-L.; Xu, Q. *Catal. Today* **2011**, *170*, 56. (d) Cao, C. Y.; Chen, C. Q.; Li, W.; Song, W. G.; Cai, W. *ChemSusChem* **2010**, *3*, 1241. (e) Metin, Ö.; Mazumder, V.; Özkar, S.; Sun, S. *J. Am. Chem. Soc.* **2010**, *132*, 1468. (f) Metin, Ö.; Özkar, S.; Sun, S. *Nano Res.* **2010**, *3*, 676. (g) Hamilton, C. W.; Baker, R. T.; Staubitz, A.; Manners, I. *Chem. Soc. Rev.* **2009**, *38*, 279. (h) Yan, J.-M.; Zhang, X.-B.; Han, S.; Shioyama, H.; Xu, Q. *Angew. Chem., Int. Ed.* **2008**, *47*, 2287. (i) Kalidindi, S. B.; Indirani, M.; Jagirdar, B. R. *Inorg. Chem.* **2008**, *47*, 7424. (j) Chandra, M.; Xu, Q. *J. Power Sources* **2007**, *168*, 135. (k) Keaton, R. J.; Blacquiere, J. M.; Baker, R. T. *J. Am. Chem. Soc.* **2007**, *129*, 1844.

(16) (a) Kim, S.-K.; Kim, T.-J.; Kim, T.-Y.; Lee, G.; Park, J. T.; Nam, S. W.; Kang, S. O. *Chem. Commun.* **2012**, *48*, 2021. (b) Zhong, R.-Q.; Zou, R.-Q.; Nakagawa, T.; Janicke, M.; Semelsberger, T. A.; Burrell, A. K.; Del Sesto, R. E. *Inorg. Chem.* **2012**, *51*, 2728. (c) Gadipelli, S.; Ford, J.; Zhou, W.; Wu, H.; Udovic, T. J.; Yildirim, T. *Chem.—Eur. J.* **2011**, *17*, 6043. (d) Kim, S.-K.; Han, W.-S.; Kim, T.-J.; Kim, T.-Y.; Nam, S. W.; Mitoraj, M.; Piekos, L..; Michalak, A.; Hwang, S. J.; Kang, S. O. *J. Am. Chem. Soc.* **2010**, *132*, 9954. (e) Li, Z.; Zhu, G.; Lu, G.; Qiu, S.; Yao, X. *J. Am. Chem. Soc.* **2010**, *132*, 1490. (f) He, T.; Xiong, Z.; Wu, G.; Chu, H.; Wu, C.; Zhang, T.; Chen, P. *Chem. Mater.* **2009**, *21*, 2315. (g) Gutowska, A.; Li, L.; Shin, Y.; Wang, C. M.; Li, X. S.; Linehan, J. C.; Smith, R. S.; Kay, B. D.; Schmid, B.; Shaw, W.; Gutowski, M.; Autrey, T. *Angew. Chem., Int. Ed.* **2005**, *44*, 3578.

(17) (a) Ye, J.-Y.; Liu, C.-J. *Chem. Commun.* **2011**, *47*, 2167. (b) Zhao, Y.; Padmanabhan, M.; Gong, Q.; Tsumori, N.; Xu, Q.; Li, J. *Chem. Commun.* **2011**, *47*, 6377. (c) Haruta, M.; Kobayashi, T.; Sano, H.; Yamada, N. *Chem. Lett.* **1987**, 405.

(18) Prashar, A. K.; Mayadevi, S.; Rajamohanan, P. R.; Devi, R. N. *Appl. Catal., A* **2011**, *403*, 91.

13929

dx.doi.org/10.1021/ja3043905 | *J. Am. Chem. Soc.* 2012, 134, 13926–13929